Hindawi Publishing Corporation
Advances in Materials Science and Engineering
Volume 2016, Article ID 6987218, 7 pages
http://dx.doi.org/10.1155/2016/6987218

Research Article

Studies on Characterization of Bovine Hydroxyapatite/$CaTiO_3$ Biocomposites

Suat Ozturk and Mehmet Yetmez

Department of Mechanical Engineering, Bulent Ecevit University, 67100 Zonguldak, Turkey

Correspondence should be addressed to Mehmet Yetmez; yetmez@beun.edu.tr

Received 15 July 2016; Revised 7 September 2016; Accepted 15 September 2016

Academic Editor: Charles C. Sorrell

Sintering effects and mechanical properties of bovine hydroxyapatite/$CaTiO_3$ composites are investigated for different $CaTiO_3$ ratios. Results indicate that densities of the biocomposites increase while total porosities of those decrease with increasing sintering temperature. Moreover, modulus of elasticity and microhardness increase with increasing sintering temperature. However, values of both toughness and fracture toughness of the biocomposites generally rise with increasing sintering temperature except for 1300°C.

1. Introduction

Calcium phosphate bioceramics, namely, hydroxyapatite (HA, $Ca_{10}(PO_4)_6(OH)_2$), are well-known materials for bone reconstruction. HA is mostly used to fill in and to construct bone and teeth in medicine. Generally, HA is mixed or coated by other minerals and materials to rehabilitate its brittleness and low strength [1–3]. $CaTiO_3$ is auxiliary to form apatite and prevents HA from dissolving in acidic tissue environment. Moreover, materials including $CaTiO_3$ do not give any negative reaction with tissues and connect better to osteoblast cells with respect to HA and titanium. For these reasons, it is thought that $CaTiO_3$-HA composites can show good biocompatibility, bioactivity, osteoconductivity, and mechanical performance [4–10]. More $CaTiO_3$ addition than 60% to HA raises AC conductivity and the dielectric constant of $CaTiO_3$-HA composites [11]. Linh et al. have found that 30 wt% $CaTiO_3$ with 70 wt% HA has a better biocompatibility and mechanical strength with respect to varying HA contents (0%, 50%, 70%, and 100%) [12]. Studies indicate that (i) BHA is more economic than synthetic HA [13–15] and (ii) characterization and understanding of mechanical behavior of BHA are still an open area in biomaterials world [16]. In particular, there is scarcely any study related to influence of sintering temperature on mechanical properties of $CaTiO_3$-HA composites in the literature.

The aim of this study is to determine the sintering effects and mechanical properties of bovine hydroxyapatite/$CaTiO_3$ composites with different weight of $CaTiO_3$. For this purpose, HA bioceramic material produced from bovine bones (i.e., bovine hydroxyapatite, BHA) is considered.

2. Material and Methods

BHA obtained from compact section of a bovine femur may be a biomechanically preferable material for medical applications, especially orthopaedic applications [17]. It is generally known that small pieces of cleared femur bone are treated with NaOH to remove organic compounds. After completing deproteinization process [18], the BHA powder is produced by the method of [19]. Final BHA particle size is around 100 μm. Cylindrical BHA/$CaTiO_3$ samples are put together by mixing dry BHA and $CaTiO_3$ (Sigma-Aldrich Chemie GmbH, Taufkirchen, Germany). The catalog number for $CaTiO_3$ is #372609. According to the British Standard BS 7253, pellets (approximately 10 mm in diameter and 12 mm in height) are prepared by using uniaxial cold pressing in hardened steel dies under 350 MPa.

Due to the fact that sintering temperature may increase solubility and mechanical strength of general calcium phosphates [20], 4 h may be a long soak time for HA to decrease solubility with respect to high crystallinity. In addition to soak

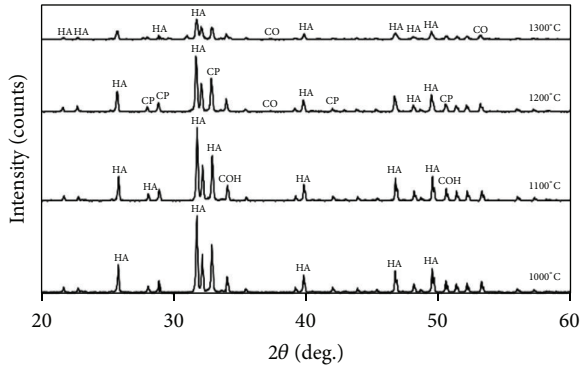

Figure 1: X-ray diffractograms of BHA samples sintered at different temperatures.

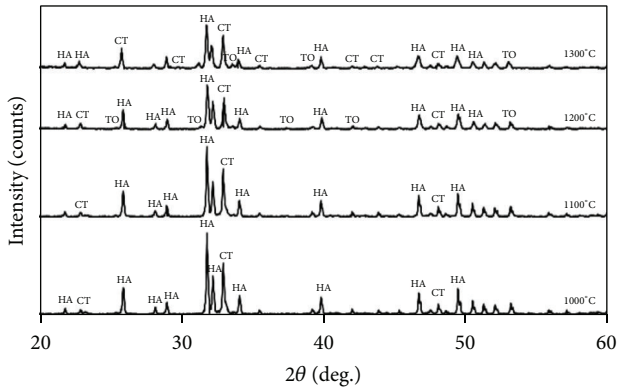

Figure 2: X-ray diffractograms of 5BHA composites sintered at different temperatures.

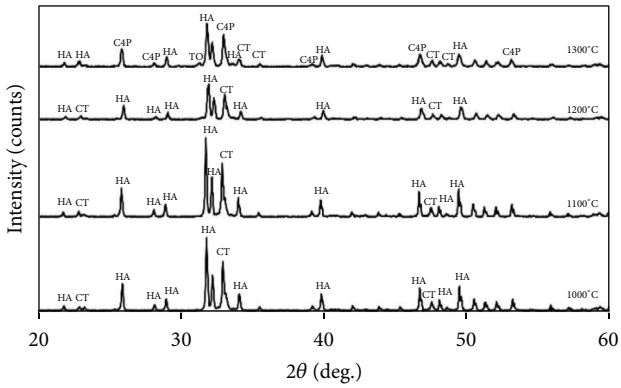

Figure 3: X-ray diffractograms of 10BHA composites sintered at different temperatures.

time effect, however, in order to decrease the effect of thermal stress on HA, heating rate is not to be exceeding 5°C/min [21]. Therefore, while one study on HA considers heating rate of 2°C/min for 2 h [22], others regard that of 1°C/min for 3 h [21] or that of 4°C/min for 4 h [23]. Consequently, this study regards that the pressed samples are sintered in an open atmospheric furnace at different temperatures, specifically 1000, 1100, 1200, and 1300°C, for 4 h under a heating rate

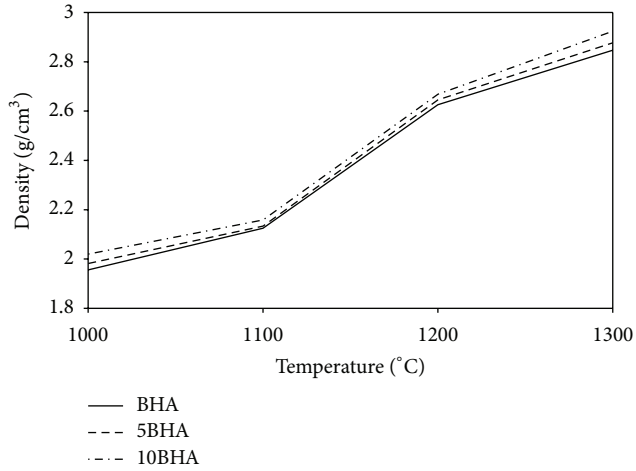

Figure 4: Variation of density of sintered BHA, 5BHA, and 10BHA composites at different sintering temperature.

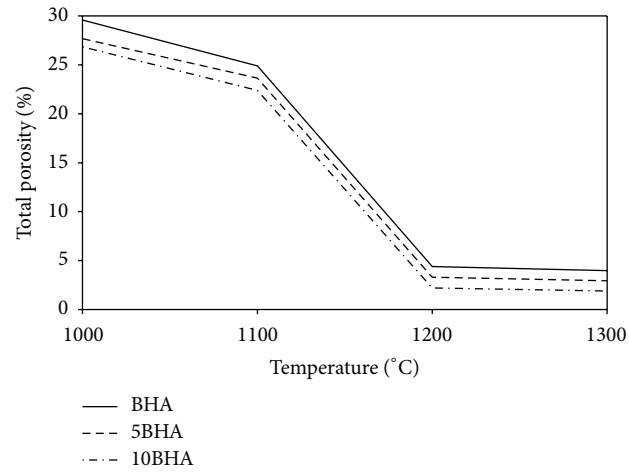

Figure 5: Variation of total porosity of sintered BHA, 5BHA, and 10BHA composites at different sintering temperature.

of 4°C/min. For each temperature, 12 cylindrical samples of hydroxyapatite and hydroxyapatite/$CaTiO_3$ biocomposites are produced. Three testing groups are prepared as BHA (100 wt% BHA), 5BHA (95 wt% BHA and 5 wt% $CaTiO_3$), and 10BHA (90 wt% BHA and 10 wt% $CaTiO_3$).

Density of the sintered samples is determined by the Archimedes method. Porosity measurements are carried out with a mercury porosimeter (Quantachrome Corporation, Poremaster 60, USA). Crystalline phases identification is realised with an X-ray diffractometer (Rigaku Ultima-IV, Japan) with scanning rate of 0.5 degrees/min and scanning interval of 20–60 degrees. Microstructural analysis is completed by a scanning electron microscope (QUANTA 400F Field Emission SEM, USA) for 1000 and 10000 magnifications. From the micromechanical point of view, measurements of Vickers microhardness and modulus of elasticity are carried out in a microhardness testing machine (CSM Instrument, Switzerland), using 100 g load applied for 20 s (dwell time). Microhardness testing machine is also used to

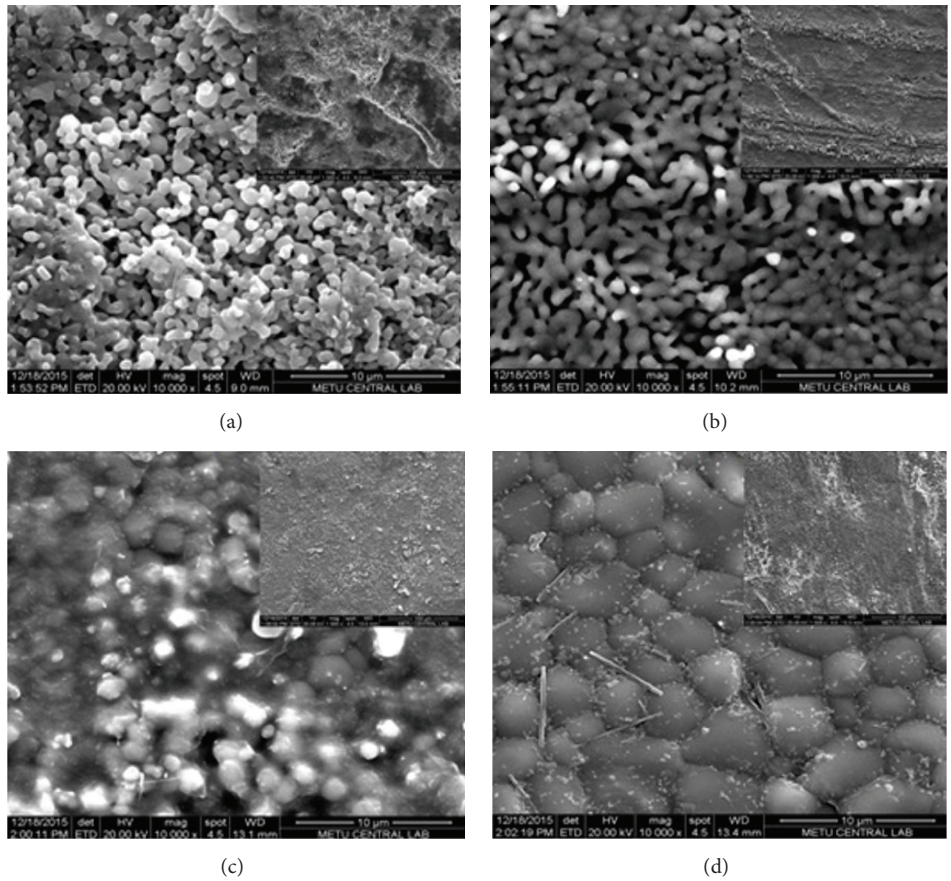

Figure 6: Microstructures of BHA samples sintered at (a) 1000°C, (b) 1100°C, (c) 1200°C, and (d) 1300°C at low (×1000, insets) and high (×10000, main images) magnifications.

get the traces of the indents and the length of the fractures to make the fracture toughness calculations under 10 kg load applied for 20 s. For the macromechanical tests, a universal tensile testing machine (Zwick, Germany) is utilized to obtain maximum compressive strength and toughness under a loading rate of 0.5 mm/min.

The experimental evaluations are analyzed with a general purpose statistical data analysis program WINKS SDA (Version 6.0.91 Professional Ed., TexaSoft, Houston, TX). In these statistical analyses, independent group t-test/ANOVA with comparison type Newman-Keuls and any difference at the 5% level are considered.

Table 1: Components, abbreviations, and compound names in X-ray diffractogram figures.

Component	Abbreviation	Compound name
$CaTiO_3$	CT	Calcium titanate
$Ca_{10}(PO_4)_6(OH)_2$	HA	Hydroxyapatite
$Ca(OH)_2$	COH	Calcium hydroxide
CaP_3	CP	Calcium phosphide
TiO_2	TO	Titanium dioxide
CaO	CO	Calcium oxide
$Ca_4P_2O_9$	C4P	Tetracalcium phosphate

3. Results and Discussion

Table 1 represents component and compound name for abbreviations used in X-ray diffractogram figures. The X-ray diffractograms of BHA composites sintered at 1000, 1100, 1200, and 1300°C are shown in Figure 1. Increment of sintering temperature seems not to affect the amount of HA. CO and CP compounds come up at 1200°C and 1300°C. COH takes place at 1100°C and disappears later. The X-ray diffractograms of 5BHA composites sintered at 1000, 1100, 1200, and 1300°C are shown in Figure 2. The amount of HA stays like same with increasing sintering temperature. CT reduces after 1200°C and TO takes place.

The X-ray diffractograms of 10BHA composites sintered at 1000, 1100, 1200, and 1300°C are shown in Figure 3. It is seen that C4P and TO come up at 1300°C and CT decreases. From all the X-ray diffractograms, it is determined that composite mixtures are pure (just including BHA and $CaTiO_3$ components).

Mean density and total porosity values of sintered samples are given in Figures 4 and 5. From these two figures, one can say that densities of samples increase with increasing

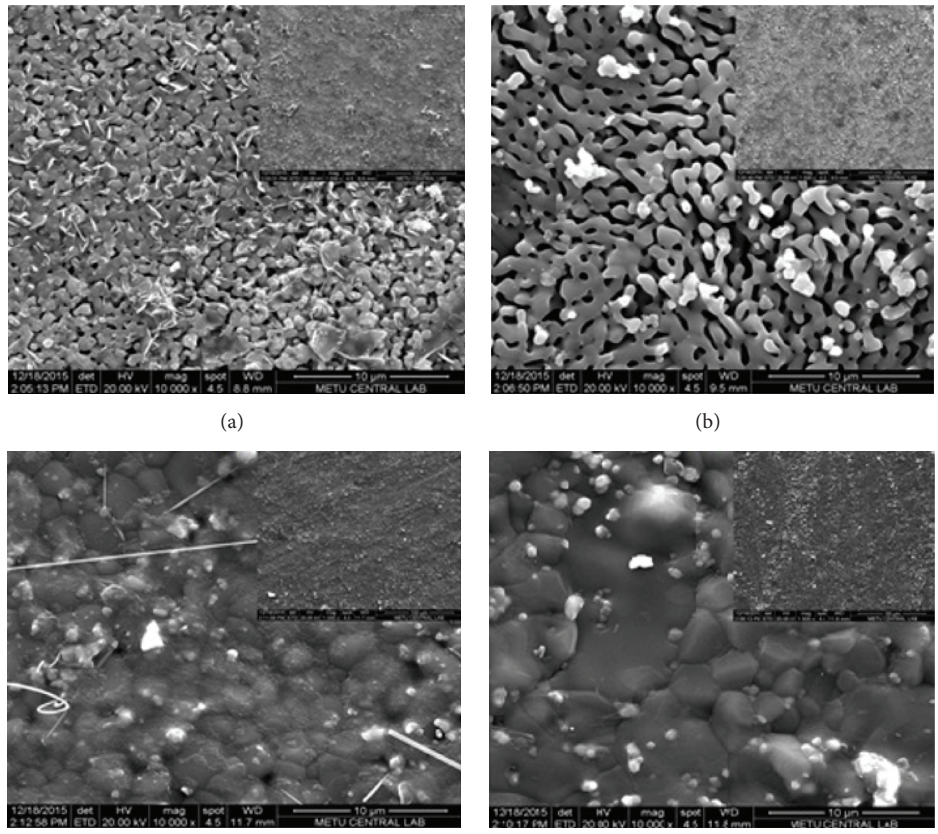

Figure 7: Microstructures of 5BHA composites sintered at (a) 1000°C, (b) 1100°C, (c) 1200°C, and (d) 1300°C at low (×1000, insets) and high (×10000, main images) magnifications.

sintering temperature and the highest density belongs to 10BHA followed by 5BHA and BHA composites in the decreasing order. The ranking of porosity from the highest to the lowest is at the order of BHA, 5BHA, and 10BHA. The total porosities reduce with increasing sintering temperature for three different compositions. As a result, it is obvious that density is supposed to rise while porosity decreases.

The microstructures of sintered BHA, 5BHA, and 10BHA samples are given in Figures 6–8. Generally, it is determined that the mixtures of $CaTiO_3$ and BHA are homogeneous and the increment of sintering temperature increases fusion among the mixture grains and diminishes porosity. There are the wide pores among grains at 1000°C for all composites. One can observe that the needle-like crystalline aggregates in Figure 6(d). It may be discussed that becoming more crystalline particles is due to the soaking time of 4 h. In Figures 7 and 8, $CaTiO_3$ pieces can be seen at 1000°C. The small pores among grains are still available and the fusing and merging among grains rise at 1100°C. The pores among the fused and merged grains disappear at 1200°C. Finally, the small merged grains unite with each other and create bigger grains at 1300°C.

Figures 9 and 10 present variations of modulus of elasticity and Vickers microhardness of BHA, 5BHA, and 10BHA ceramic samples with respect to sintering temperature. Modulus of elasticity rises with the increment of sintering temperature. The ranking from the highest to lowest according to elasticity modulus values is at the order of BHA, 5BHA, and 10BHA except for 1100°C before. The behavior of microhardness is supposed to show resemblance to that of modulus of elasticity as in this study. BHA belonging to the highest microhardness values is followed by 5BHA and 10BHA in the ranking like modulus of elasticity. Statistically, results of analysis of modulus of elasticity are as follows. (i) At the 0.05 significance level, groups BHA at 1000 and 1100°C are not significantly different, (ii) all four groups of 5BHA are significantly different from each other, and (iii) groups 10BHA at 1000 and 1100°C are not significantly different. And the results of statistical analysis of Vickers hardness are as follows. (i) At the 0.05 significance level, groups BHA at 1000 and 1100°C are not significantly different and (ii) groups of 5BHA and 10BHA at 1000 and 1100°C are not significantly different.

Variation of toughness of the sintered ceramics is represented in Figure 11. The toughness values rise with increasing sintering temperatures except for 10BHA at 1300°C. The highest toughness values mostly belong to BHA followed by 10BHA and 5BHA. The addition of 5% and 10% $CaTiO_3$ to BHA seems to decrease toughness. It is seen that higher

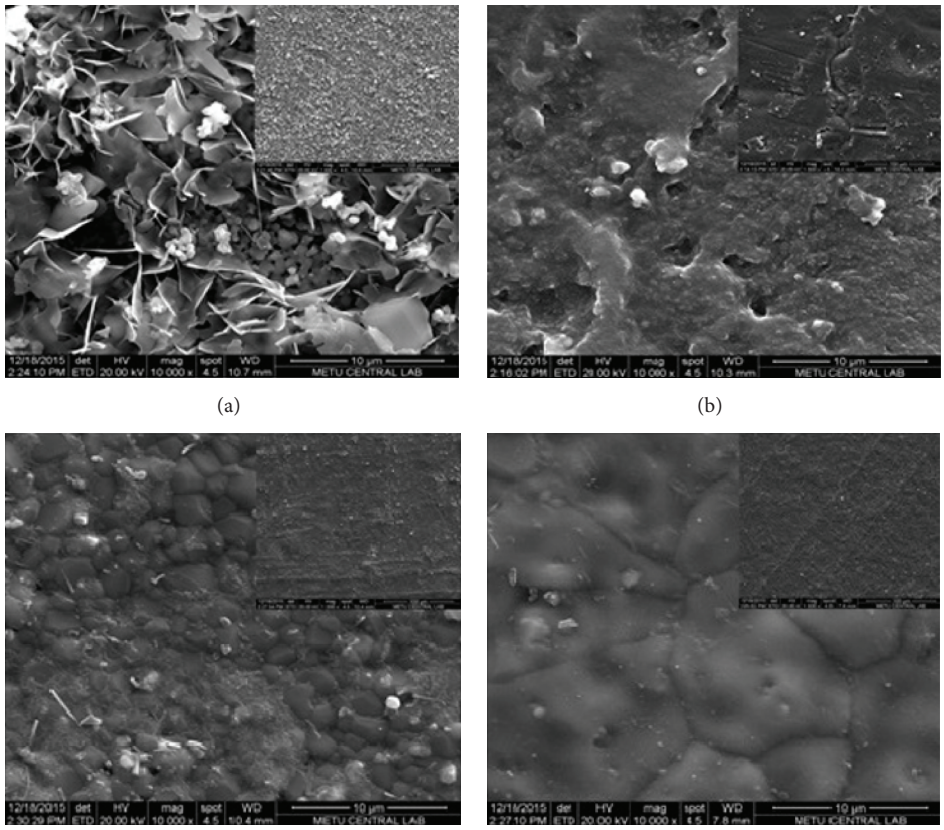

Figure 8: Microstructures of 10BHA composites sintered at (a) 1000°C, (b) 1100°C, (c) 1200°C, and (d) 1300°C at low (×1000, insets) and high (×10000, main images) magnifications.

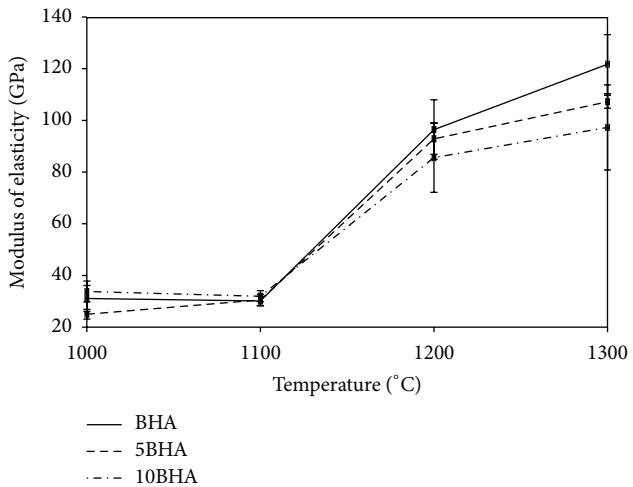

Figure 9: Variation of modulus of elasticity of BHA, 5BHA, and 10BHA composites at different sintering temperature.

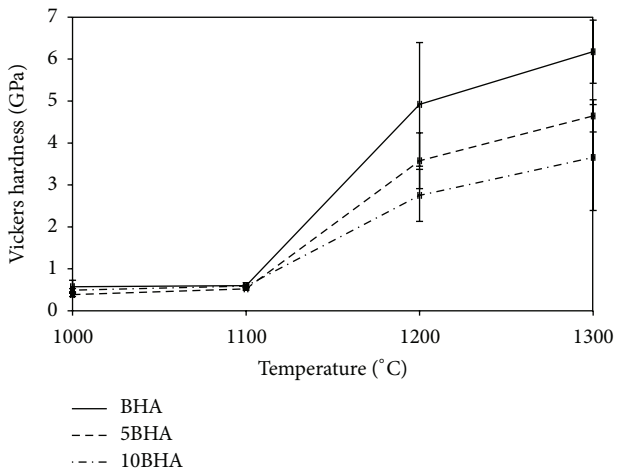

Figure 10: Variation of microhardness of BHA, 5BHA, and 10BHA composites at different sintering temperature.

toughness values can be obtained with more $CaTiO_3$ addition than 10% to BHA. Statistically, results of analysis of toughness are as follows: (i) At the 0.05 significance level, all four groups of BHA are significantly different from each other, (ii) groups 5BHA at 1100 and 1200°C are not significantly different, and (iii) all four groups of 10BHA are significantly different from each other.

Characteristic crack pattern and mean fracture toughness values of sintered samples are given in Figures 12 and 13,

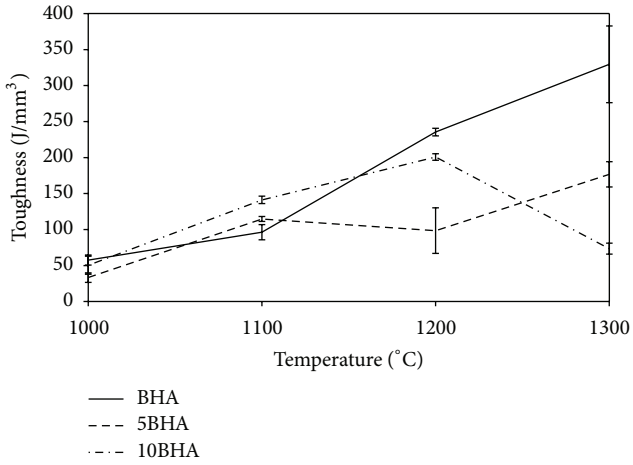

Figure 11: Variation of toughness of BHA, 5BHA, and 10BHA composites at different sintering temperature.

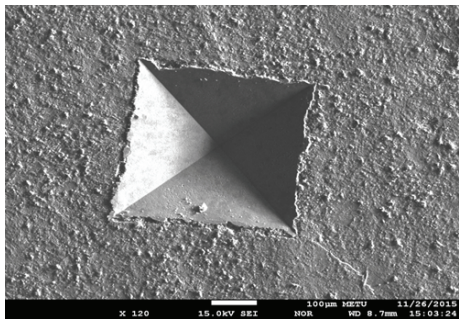

Figure 12: A crack initiated from the corner of a Vickers indent for a 5BHA composite sintered at 1300°C.

respectively. Fracture toughness values are calculated by using (1), where K_{IC}, ξ, E, H, P, and c_o are fracture toughness (MPa·m$^{0.5}$), constant ($\xi = 0.016$), modulus of elasticity (N/m^2), Vickers hardness, N/m^2, load (kg·m/s^2), and fracture length (m), respectively [24].

$$K_{IC} = \xi \left[\frac{E}{H}\right]^{0.5} \frac{P}{c_o^{1.5}}. \quad (1)$$

Figure 13 indicates that (i) the fracture toughness increases with increasing sintering temperature except for 1300°C; (ii) the ranking of fracture toughness from the highest to the lowest is in the order of BHA, 10BHA, and 5BHA; BHA possesses the highest fracture toughness at 1200°C; (iii) there are reductions of BHA and 10BHA after 1200°C in contrast to 5BHA. It is discussed that the fracture toughness of composites including more than 10% of $CaTiO_3$ addition may exceed the fracture toughness of BHA. Results of statistical analysis of fracture toughness are as follows: (i) At the 0.05 significance level, groups of BHA at 1000, 1100, and 1300°C are not significantly different, (ii) groups 5BHA at 1100 and 1200°C are not significantly different, and (iii) groups 10BHA at 1000 and 1300°C are not significantly different.

Thus, with respect to the consolidation of 10BHA, good sintering regime can be observed at 1200°C, which is reflected

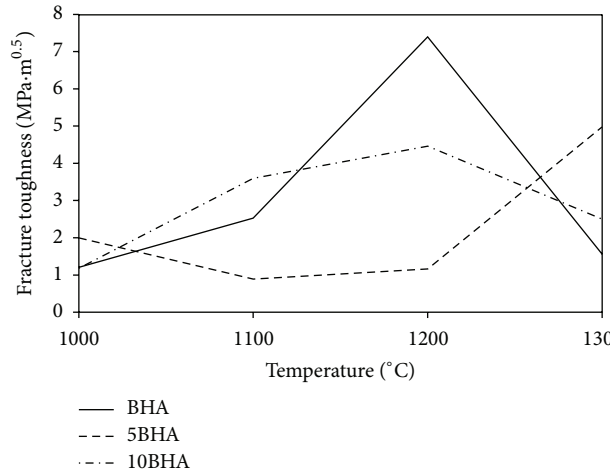

Figure 13: Variation of fracture toughness of BHA, 5BHA, and 10BHA composites at different sintering temperature.

in the high values of toughness and fracture toughness. The grains of 10BHA gradually grow at 1300°C, where that material with large grains is more fragile than the materials of all the other groups. Moreover, for all groups, due to the fact that there is no observation of intergranular/intragranular crack growth, increasing sintering temperature in the range of 1100–1300°C increases values of modulus of elasticity and Vickers hardness. Therefore, it can be discussed that 10BHA in the range of 1100–1200°C sintering temperature may be suitable for the biomedical applications with possible granular crack existence.

4. Conclusions

The total porosities reduce with increasing sintering temperature for three different compositions which are ranking from the highest to the lowest at the order of BHA, 5BHA, and 10BHA. On the contrary, the densities of samples increase with increasing sintering temperature. Increment of sintering temperature seems not to affect the amount of HA. CO and CP compounds come up at 1200°C and 1300°C in BHA X-rays. CT reduces after 1200°C and TO takes place in 5BHA X-rays. C4P and TO come up at 1300°C and CT decreases in 10BHA X-rays and all composite mixtures are pure. The mixtures of $CaTiO_3$ and BHA are homogeneous and the increment of sintering temperature increases fusing and melting among the mixture grains and diminishes porosity.

Modulus of elasticity and microhardness rise with the increment of sintering temperature. The ranking to the lowest from the highest is at the order of BHA, 5BHA, and 10BHA for both. The fracture toughness and toughness of composites generally increase with increasing sintering temperature except for 1300°C. The ranking for both from the highest to the lowest is in the order of BHA, 10BHA, and 5BHA. It is supposed that more $CaTiO_3$ than 10% be added in BHA to exceed the fracture toughness and toughness values of BHA.

Competing Interests

The authors declare that they have no competing interests regarding the publication of this paper.

References

[1] M. Aminzare, A. Eskandari, M. H. Baroonian et al., "Hydroxyapatite nanocomposites: synthesis, sintering and mechanical properties," *Ceramics International*, vol. 39, no. 3, pp. 2197–2206, 2013.

[2] S. Nath, R. Tripathi, and B. Basu, "Understanding phase stability, microstructure development and biocompatibility in calcium phosphate-titania composites, synthesized from hydroxyapatite and titanium powder mix," *Materials Science and Engineering: C*, vol. 29, no. 1, pp. 97–107, 2009.

[3] C. S. Ciobanu, S. L. Iconaru, I. Pasuk et al., "Structural properties of silver doped hydroxyapatite and their biocompatibility," *Materials Science and Engineering C*, vol. 33, no. 3, pp. 1395–1402, 2013.

[4] W. Dong, B. Song, W. Meng, G. Zhao, and G. Han, "A simple solvothermal process to synthesize $CaTiO_3$ microspheres and its photocatalytic properties," *Applied Surface Science*, vol. 349, pp. 272–278, 2015.

[5] M. A. Ramírez, R. Parra, M. M. Reboredo, J. A. Varela, M. S. Castro, and L. Ramajo, "Elastic modulus and hardness of $CaTiO_3$, $CaCu_3Ti_4O_{12}$ and $CaTiO_3/CaCu_3Ti_4O_{12}$ mixture," *Materials Letters*, vol. 64, no. 10, pp. 1226–1228, 2010.

[6] J. Zhuang, Q. Tian, S. Lin, W. Yang, L. Chen, and P. Liu, "Precursor morphology-controlled formation of perovskites $CaTiO_3$ and their photo-activity for As(III) removal," *Applied Catalysis B: Environmental*, vol. 156-157, pp. 108–115, 2014.

[7] C. Ergun, "Novel machinable calcium phosphate/$CaTiO_3$ composites," *Ceramics International*, vol. 37, no. 3, pp. 1143–1146, 2011.

[8] A. K. Dubey, B. Basu, K. Balani, R. Guo, and A. S. Bhalla, "Multifunctionality of perovskites $BaTiO_3$ and $CaTiO_3$ in a composite with hydroxyapatite as orthopedic implant materials," *Integrated Ferroelectrics*, vol. 131, no. 1, pp. 119–126, 2011.

[9] S. Wu, B. Tu, J. Lin et al., "Evaluation of the biocompatibility of a hydroxyapatite-$CaTiO_3$ coating in vivo," *Biocybernetics and Biomedical Engineering*, vol. 35, no. 4, pp. 296–303, 2015.

[10] A. K. Dubey, G. Tripathi, and B. Basu, "Characterization of hydroxyapatite-perovskite ($CaTiO_3$) composites: phase evaluation and cellular response," *Journal of Biomedical Materials Research B: Applied Biomaterials*, vol. 95, no. 2, pp. 320–329, 2010.

[11] A. K. Dubey, P. K. Mallik, S. Kundu, and B. Basu, "Dielectric and electrical conductivity properties of multi-stage spark plasma sintered HA-$CaTiO_3$ composites and comparison with conventionally sintered materials," *Journal of the European Ceramic Society*, vol. 33, no. 15-16, pp. 3445–3453, 2013.

[12] N. T. B. Linh, D. Mondal, and B. T. Lee, "In vitro study of $CaTiO_3$–hydroxyapatite composites for bone tissue engineering," *ASAIO Journal: Tissue Engineering/Biomaterials*, vol. 60, no. 6, pp. 722–729, 2014.

[13] C. Y. Ooi, M. Hamdi, and S. Ramesh, "Properties of hydroxyapatite produced by annealing of bovine bone," *Ceramics International*, vol. 33, no. 7, pp. 1171–1177, 2007.

[14] M. K. Herliansyah, M. Hamdi, A. Ide-Ektessabi, M. W. Wildan, and J. A. Toque, "The influence of sintering temperature on the properties of compacted bovine hydroxyapatite," *Materials Science and Engineering: C*, vol. 29, no. 5, pp. 1674–1680, 2009.

[15] A. Niakan, S. Ramesh, P. Ganesan et al., "Sintering behaviour of natural porous hydroxyapatite derived from bovine bone," *Ceramics International*, vol. 41, no. 2, pp. 3024–3029, 2015.

[16] H. Asgharzadeh Shirazi, M. R. Ayatollahi, and B. Beigzadeh, "Preparation and characterisation of hydroxyapatite derived from natural bovine bone and PMMA/BHA composite for biomedical applications," *Materials Technology: Advanced Performance Materials*, vol. 31, no. 8, pp. 448–453, 2016.

[17] M. Yetmez and S. Gürses, "Physical and mechanical properties of a compact bone according to its hierarchical structure," in *Proceedings of the 4th National Biomechanics Conference*, pp. 496–505, Erzurum, Turkey, October 2008 (Turkish).

[18] R. Uklejewski, M. Winiecki, G. Musielak, and R. Tokłowicz, "Effectiveness of various deproteinization processes of bovine cancellous bone evaluated via mechano-biostructural properties of produced osteoconductive biomaterials," *Biotechnology and Bioprocess Engineering*, vol. 20, no. 2, pp. 259–266, 2015.

[19] F. N. Oktar, K. Kesenci, and E. Pişkin, "Characterization of processed tooth hydroxyapatite for potential biomedical implant applications," *Artificial Cells, Blood Substitutes, and Biotechnology*, vol. 27, no. 4, pp. 367–379, 1999.

[20] M. N. Helmus and K. Tweden, *Encyclopedic Handbook of Biomaterials and Bioengineering*, Marcel Dekker, New York, NY, USA, 1995.

[21] O. Prokopiev and I. Sevostianov, "Dependence of the mechanical properties of sintered hydroxyapatite on the sintering temperature," *Materials Science and Engineering: A*, vol. 431, no. 1-2, pp. 218–227, 2006.

[22] G. Muralithran and S. Ramesh, "The effects of sintering temperature on the properties of hydroxyapatite," *Ceramics International*, vol. 26, no. 2, pp. 221–230, 2000.

[23] G. Goller, F. N. Oktar, S. Agathopoulos et al., "Effect of sintering temperature on mechanical and microstructural properties of bovine hydroxyapatite (BHA)," *Journal of Sol-Gel Science and Technology*, vol. 37, no. 2, pp. 111–115, 2006.

[24] I. L. Denry and J. A. Holloway, "Elastic constants, Vickers hardness, and fracture toughness of fluorrichterite-based glass-ceramics," *Dental Materials*, vol. 20, no. 3, pp. 213–219, 2004.